



Contents lists available at ScienceDirect

Science Bulletin

journal homepage: www.elsevier.com/locate/scib

Article

High conductive graphene assembled films with porous micro-structure for freestanding and ultra-low power strain sensors

Zhe Wang^{a,b,1}, Peng Li^{a,1}, Rongguo Song^a, Wei Qian^a, Huang Zhou^c, Qianlong Wang^a, Yong Wang^c, Xianci Zeng^a, Lin Ren^{a,*}, Shilin Yan^b, Shichun Mu^c, Daping He^{a,c,*}

^aHubei Engineering Research Center of RF-Microwave Technology and Application, School of Science, Wuhan University of Technology, Wuhan 430070, China

^bHubei Key Laboratory of Theory and Application of Advanced Materials Mechanics, School of Science, Wuhan University of Technology, Wuhan 430070, China

^cState Key Laboratory of Advanced Technology for Materials Synthesis and Processing, Wuhan University of Technology, Wuhan 430070, China

ARTICLE INFO

Article history:

Received 8 March 2020

Received in revised form 15 April 2020

Accepted 26 April 2020

Available online xxxxx

Keywords:

Strain sensor

High conductivity

Graphene assembled film

Freestanding

Ultra-low power consumption

ABSTRACT

Graphene emerges as an ideal material for constructing high-performance strain sensors, due to its superior mechanical property and high conductivity. However, in the process of assembling graphene into macroscopic materials, its conductivity decreases significantly. Also, tedious fabrication process hinders the application of graphene-based strain sensors. In this work, we report a freestanding graphene assembled film (GAF) with high conductivity ($(2.32 \pm 0.08) \times 10^5 \text{ S m}^{-1}$). For the sensitive materials of strain sensors, it is higher than most of reported carbon nanotube and graphene materials. These advantages enable the GAF to be an ultra-low power consumption strain sensor for detecting airflow and vocal vibrations. The resistance of the GAF remains unchanged with increasing temperature (20–100 °C), exhibiting a good thermal stability. Also, the GAF can be used as a strain sensor directly without any flexible substrates, which greatly simplifies the fabrication process in comparison with most reported strain sensors. Additionally, the GAF used as a pressure sensor with only $\sim 4.7 \mu\text{W}$ power is investigated. This work provides a new direction for the preparation of advanced sensors with ultra-low power consumption, and the development of flexible and energy-saving electronic devices.

© 2020 Science China Press. Published by Elsevier B.V. and Science China Press. All rights reserved.

1. Introduction

Flexible strain sensors, which are able to transform the stimulus of mechanical deformation into the signals of electrical shifts [1–3], have received increasing attention for their widespread applications on wearable devices [4–6], artificial skins [7,8], human-machine interactions [9,10], robotics [11–13], and speech rehabilitation trainings [14,15]. Flexible sensors can be divided into several types based on the working principle, such as triboelectric-type, capacitance-type, piezoelectric-type, and resistance-type [1,16]. Thereof, the resistance-type sensor is usually prepared by a simple process, but possesses an efficient effect in receiving the signals of electrical shifts. Thus, many metallic materials and conductive polymers have been tried to obtain effective resistance-type sensors. However, large density, inferior chemical stability and low flexibility for metallic materials and

relative poor electrical conductivity for conductive polymers prohibit their practical applications [1].

Graphene material is a promising candidate for resistance-type sensors on account of its extraordinary flexibility [17,18], lightweight [19,20], high electrical conductivity and remarkable chemical stability [1,17,21,22]. For example, Liu et al. [23] synthesized a graphene woven fabric/polydimethylsiloxane (PDMS) composite with an electrical conductivity of 273 S m^{-1} , which can be applied in detecting feeble human motions. Pan et al. [24] reported a composite film combining the as-prepared 3D graphene film with PDMS, showing the superior performance of strain sensor and outstanding stretching-releasing cycle's durability. The electrical conductivity is improved to 1160 S m^{-1} . Also, Liu et al. [25] prepared a strain sensor of fish-scale-like graphene on a pre-stretched tape with enhanced sensing range of strain and the electrical conductivity (1350 S m^{-1}). In general, the resistance-type strain sensors are based on a combination of graphene materials and other flexible substrates, including PDMS [23,24,26–28], elastic tapes [29,30], textiles [23,31,32], rubbers [33], and fibers [4,13,34,35]. However, they have limited applications due to the complex fabrication process and difficulty in integration with the manufacturing processes of electronic industries [11,36]. More importantly, the insufficient

* Corresponding authors at: Hubei Engineering Research Center of RF-Microwave Technology and Application, School of Science, Wuhan University of Technology, Wuhan 430070, China.

E-mail addresses: rln@whut.edu.cn (L. Ren), hedaping@whut.edu.cn (D. He).

¹ These authors contributed equally to this work.

electrical conductivity of the graphene and hybrid materials usually leads to high power consumption, resulting in their failure in energy requirement and mass production for strain sensors.

Herein, we propose a freestanding and low power consumption strain sensor using a highly conductive graphene assembled film (GAF). The resistance of the GAF prepared by the high-temperature treatment process remains unchanged with increasing temperature, exhibiting a good thermal stability. This advantage makes the GAF a stable strain sensor. To the best of our knowledge, the conductivity of GAF is higher than most of sensitive materials in reported carbon-based strain sensors. For example, it is 17,678% higher than the conductivity of a recently reported graphene material [25]. This renders the sensor with high performance, low applied voltage, and ultra-low power consumption. Also, the manufacturing process of GAF sensor without any soft encapsulation material or substrate, is simpler, more time-saving and economical. The GAF as a macroscopic product assembled by microscopic graphene sheets, is suitable for industry manufacturing process due to its good processability and compatibility. This work provides a window to develop substrate-free and energy-saving electronic devices.

2. Experimental

2.1. Preparation of GAF

Graphene oxide (GO, purchased from Wuxi Chengyi Education Technology Co., Ltd.) was diluted with ultrapure water to form GO suspension with 2%–4% solid content. GO suspension was transformed into GO gel after mechanical stirring. Then GO gel was scraped smoothly onto the surface of a polyethylene terephthalate (PET) film, and GO film was obtained after drying at room temperature. The thickness of the GO film can be adjusted by controlling the thickness and number of the feeler gauge. Then the fabricated GO films were torn off from the PET films and put in an annealing furnace from room temperature to 1300 °C and held for 2 h under the protection of argon gas flow. Then the temperature was raised to 3000 °C and held for 1 h and cooled down slowly to room temperature. Thus, the GAF was obtained.

2.2. Preparation of the GAF based strain sensor

A GAF based strain sensor is composed of two copper wires, a small slice (e.g., 10 mm × 50 mm) of the GAF and silver conductive adhesive (Wuhan Double-Bond Chemical Co., Ltd.). For the better contact between the source meter and the GAF, the silver conductive adhesive was employed to tightly attach copper wires onto GAF after cured at 80 °C for the whole night.

2.3. Measurement of the relative resistance change $(R-R_0)/R_0$ of GAF based strain sensor

The current response signals of the strain sensor deformations were recorded by an Autolab PGSTAT302N electrochemical workstation in a two-electrode mode at room temperature. The relative resistance change $(R-R_0)/R_0$ of the GAF based strain sensor versus applied strain was based on the obtained current responding signals.

2.4. Measurement of the resistance of the GAF sensor under different temperature

The GAF sensor was placed on a constant temperature heating table. The resistance of the GAF sensor was tested by using a multimeter. During the testing, the temperature of the heating table

was heated from 20 to 100 °C, and the resistance of the GAF sensor was tested every time the temperature increased by 10 °C.

3. Results and discussion

The schematic of the GAF fabrication process is exhibited in Fig. 1a. Firstly, GO suspension was transformed into GO gel via mechanical stirring (the corresponding digital photo is shown in the step below). It is worth noting that GO sheets are the building blocks of the GO film. The atomic force microscope (AFM) image shows single-layer features of a GO sheet with an average thickness of ~1.2 nm (Fig. 1b). Some wrinkles can be also observed at the edge of the GO from AFM image, as further demonstrated by the transmission electron microscope (TEM) image in Fig. 1c (inset). These wrinkle structures formed by osmotic force, provide a big possibility to fabricate flexible GO films [19]. As expected, they could be achieved by coating the GO gel on a PET film with a blade, drying and then annealing at a high temperature under argon gas flow. At last, a large-size GAF with a length of 170 mm and a width of 150 mm can be obtained, indicating the big potential of GAF's scalable production.

To investigate the structural information of the GAF, X-ray diffraction (XRD) pattern was performed. In Fig. 1c, a narrow and intense (0 0 2) peak of a GAF is located at $2\theta = 26.64^\circ$, indicating that the graphitized carbon possesses an interlayer distance of $d = 3.35 \text{ \AA}$ according to Bragg equation. The graphitized structure was further confirmed by the weak D band (at 1335 cm^{-1}) and a low value of I_D/I_G (0.052) in Raman spectrum (Fig. 1d). Besides, the remarkable 2D band at 2726 cm^{-1} indicates the presence of graphene layers in GAF. The image taken by a super-large depth of field 3D microscopic system (KEYENCE, VHX-600E) reveals that the GAF possesses a rough surface structure. The electrical conductivity of such a GAF can be modulated from $(0.63 \pm 0.02) \times 10^5$ to $(2.32 \pm 0.08) \times 10^5 \text{ S m}^{-1}$ by changing the quantity and solid content of GO gel's precursor, and the thickness of GAF (Table S1 online). In terms of the conductivity of sensitive materials for sensors, GAF is 9% higher than the highest reported CNT material and 17,678% higher than the highest reported graphene material. To the best of our knowledge, the detected electrical conductivity of $(2.32 \pm 0.08) \times 10^5 \text{ S m}^{-1}$ in our work surpasses to the reported carbon-based strain sensors (Fig. 1f) [11,20,24,25,28,30,33,37–46], thus laying the foundation for low-power devices.

The porous micro-structure of the GAF is further confirmed by scanning electron microscope (SEM). As shown in Fig. 2a (top view) and b (45° top view), there are numerous micro-folds on the surface of GAF, which is consistent with the result obtained from Fig. 1e. In Fig. 2c, the yellow and blue dotted lines indicate two different directions of micro-folds. The yellow and blue arrows point to the direction in which the micro-folds are flattened. When the GAF receives an external tensile load, the protruding portions of the micro-folds are flattened to provide cushioning for the overall structure and to avoid structural damage, thus improving flexibility and mechanical stability. As shown in Fig. 2d, the GAF can be folded without any damage or breakage. Fig. 2e and f are both the cross-section views of the GAF with porous micro-structure, which is comprised of many micron-sized pores and single-layer or multilayer graphene laminates [17,47]. During the annealing process, the oxygen-containing functional groups gradually decomposed and converted into various gases, such as CO, CO₂ and H₂O (g). These gases gathered and escaped from adjacent graphene laminates to form micron-sized pores and micro-folds, which is similar to the cavity-branched structure [48]. In addition, these micron-sized pores and micro-folds render the GAF with high elongation of 6.7% at break (Fig. S1 online). The GAF with porous micro-structure exhibits excellent flexibility and

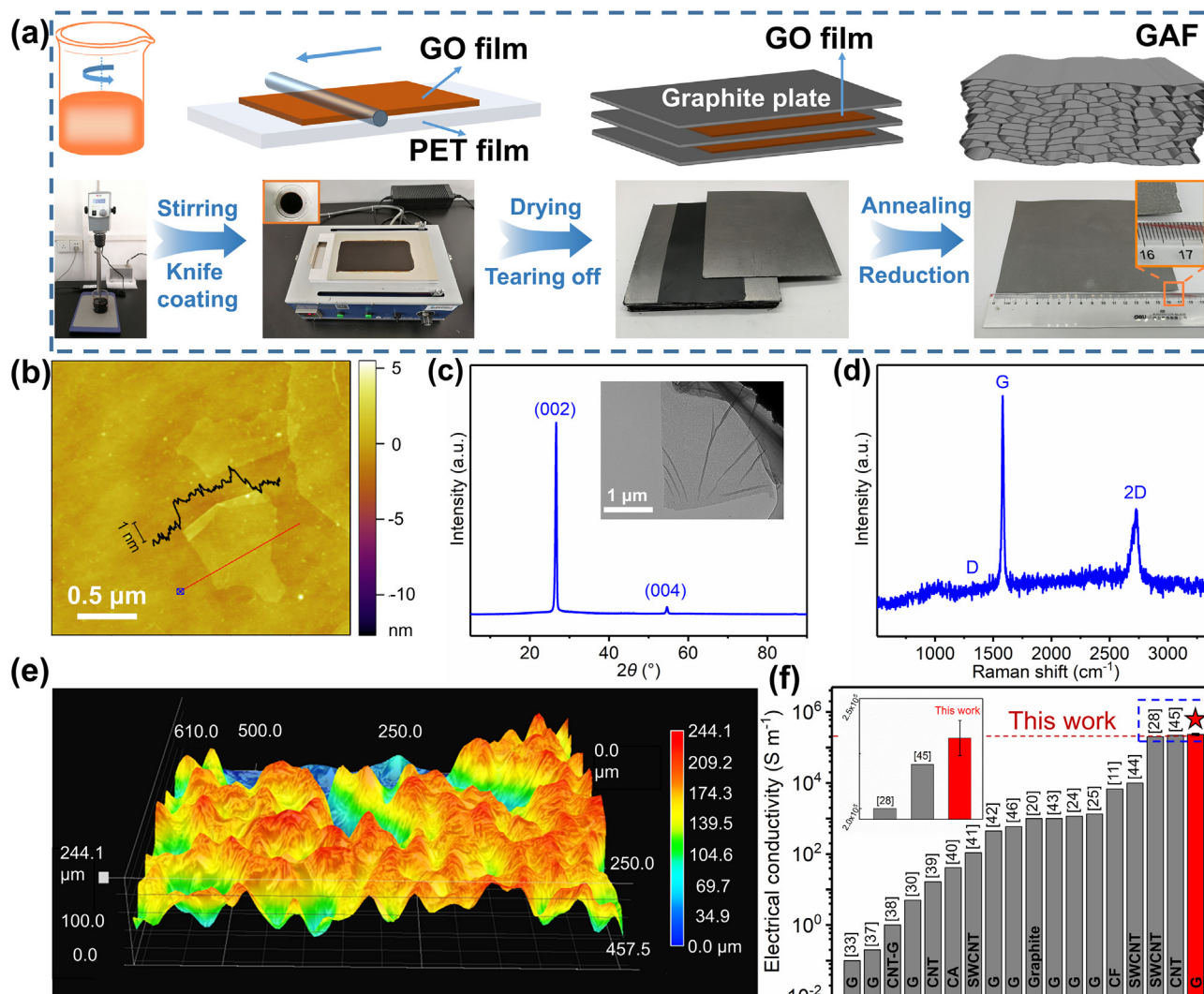


Fig. 1. (Color online) Preparation and material characterizations of the GAF. (a) The schematic of the GAF fabrication process. (b) The AFM image of GO sheets. (c) XRD pattern and (d) Raman spectrum of the GAF, the inset of (c) is the TEM image of a GO sheet. (e) The surface picture of the GAF taken by a super-large depth of field 3D microscopic system. (f) The comparison of conductivity among carbon-based strain sensors, including graphene (G), carbon nanotube (CNT), carbon aerogel (CA), carbon fiber (CF), graphite, single-walled carbon nanotube (SWCNT).

recoverability. As shown in [Movie S1](#) (online), the GAF can restore to its original state without any damage after folding and kneading. Furthermore, the GAF can maintain high electrical conductivity after 2000 bending cycles testing at a frequency of 0.5 Hz and bending angle of 0° to 150° ([Fig. 2g](#) and [S2](#) (online)), while Cu foil with the same thickness (110 μm) broke after only 23 cycles due to metal fatigue.

To explore the strain sensing performance of GAF, the electromechanical characteristics of the GAF based strain sensor were tested. As shown in [Fig. S3a](#) and [b](#) (online), four copper wire electrodes were placed on the GAF and fixed with silver conductive paste. Next, the GAF with four electrodes was flattened on the one side of a polished substrate and then encapsulated with a resin to completely fix the GAF on the surface of the substrate, which ensures the consistent deformation of the substrate and GAF when tensile loads were applied. The strain gauges were encapsulated on the other side of the substrate with the glue ([Fig. S3c](#) online). As shown in [Fig. S4](#) (online), the measuring system consists of four parts (a constant current source, a voltage recorder, a strain recorder and a universal testing machine), which is used to test the gauge factor (GF) and tensile strain stretching-releasing cycles of

a GAF based strain sensor. The GF can be calculated according to the formula $GF = ((R - R_0)/R_0)/\epsilon$, which is usually used to describe the sensitivity of a strain sensor.

As shown in [Fig. 3a](#), the sensing curve of GAF (110 μm thickness) based strain sensor can be divided into two parts ([Fig. S5](#) online). In the first part, the GF is 0.743 with linearity $R^2 = 0.925$ during the strain of 0–0.8%. This is because the resistance change of GAF is mainly related to the deformation of the porous structure surrounded by stacked graphene sheets. At this time, owing to the existing of interconnected conductive structure during the densification of GAF, the resistance change and the GF of GAF is small. In the second part, the GF is 1.934 with linearity $R^2 = 0.997$ during the strain of 0.8%–2.8%. The resistance change in GAF is mainly related to the relative sliding between adjacent stacked graphene sheets. At this time, the resistance change and the GF in GAF is more pronounced due to the enhancement of contact resistance. The GF is very close to 2.000 for the traditional metal gauges with a maximum strain of 5% [9].

The GAF strain sensor possesses the highest electrical conductivity and higher GF than many strain sensors based on graphene, CNT and other materials ([Table S2](#) online). However, the GF of the

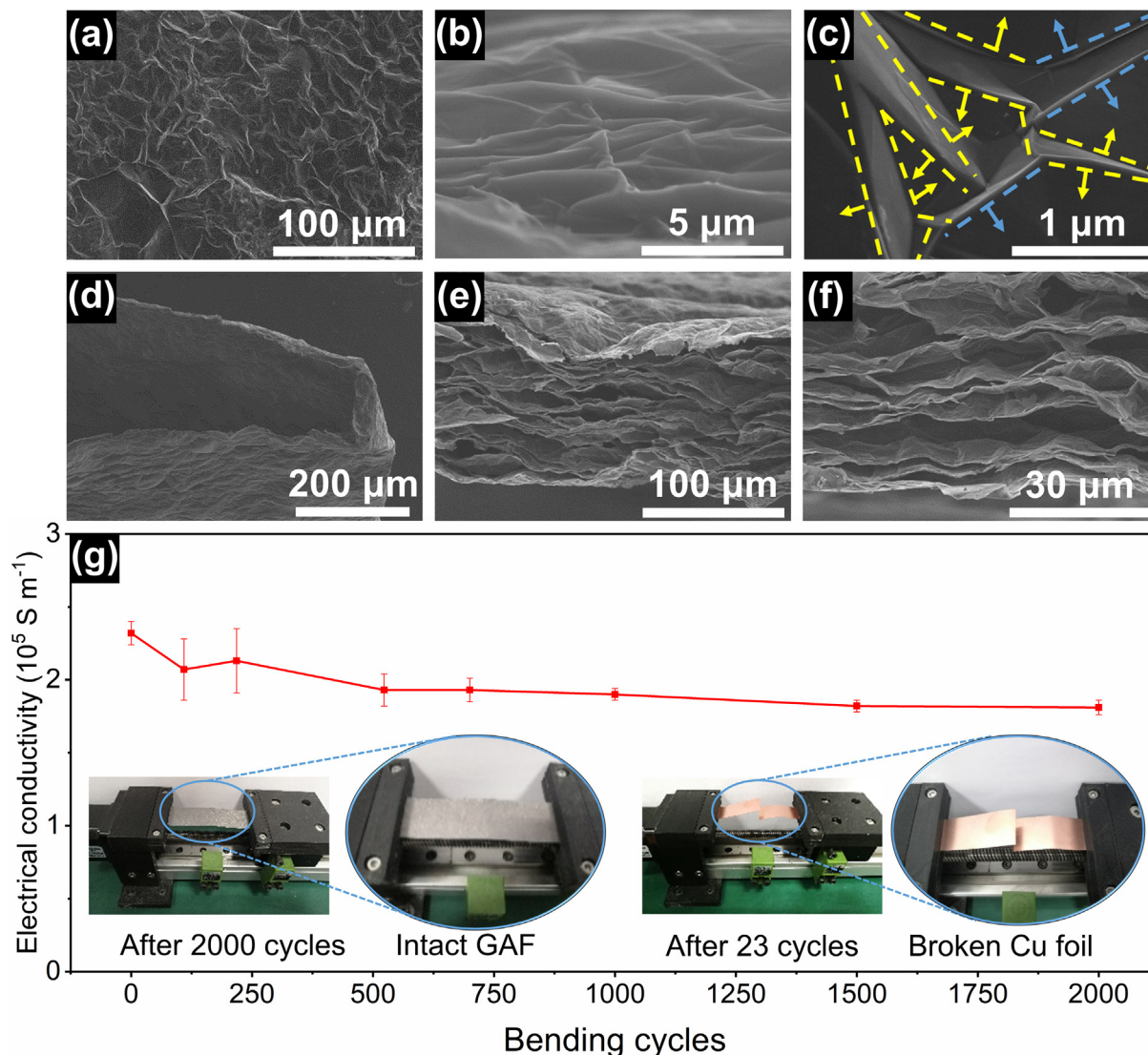


Fig. 2. (Color online) Porous micro-structure and bending stability of the GAF. (a–c) The surface SEM images of the GAF. The yellow and blue dotted lines in (c) are two different directions of micro-folds, and the yellow and blue arrows point to the directions in which the micro-folds are flattened. (d–f) The cross-sectional SEM images of the GAF. (g) The variation of electrical conductivity of GAF recorded in the 2000 bending cycles, the insets are the digital photos of intact GAF (110 μm thickness) after 2000 bending cycles and broken Cu foil (110 μm thickness) after 23 bending cycles, both at the recovering state.

GAF strain sensor still needs to be further improved (Fig. S6 online). In Fig. 3b, when the GAF based strain sensor was under different strain, the corresponding resistance variation exhibited as a step shape, and the GAF based strain sensor possesses good reproducibility. To further investigate the mechanical stability and repeatability, the whole measuring system was run cycle test for 720 cycles under 670 μE (0–2 kN tensile load), and the corresponding resistance variation is shown in Fig. 3c. Two magnified views of resistance variation during 1480.4–1632.1 s and 20,357.6–20,511.1 s are shown in the inset of Fig. 3c, exhibiting that GAF based strain sensor possesses excellent stability in the cycle test of tensile load. As shown in Fig. 3d, when the GAF based strain sensor is subjected to tensile strain, the adjacent graphene sheets slide relatively to each other, thereby increasing their contact-resistance [25].

We also explored the effect of temperature on the resistance of GAF sensor by using a multimeter. During the test, the GAF sensor was placed on a constant temperature heating table. As shown in Fig. 3e, with the temperature of the heating table was heated from 20 to 100 $^{\circ}\text{C}$, the resistance of the GAF sensor remained unchanged.

In fact, GAF that has undergone a high temperature treatment of 3000 $^{\circ}\text{C}$ has good thermal stability. The resistance of GAF does not change significantly with the increasing temperature, which is very significant for sensors.

Based on its light weight, flexibility and porous micro-structure, we also used GAF as a pressure sensor and made some preliminary explorations (Fig. S7 online). The resistance of a GAF sensor changes when subjected to pressure. The applied voltage of GAF sensor is only 0.01 V (only 1/150 of an AA-type battery working voltage of 1.5 V theoretically), which is much less than the applied voltage (typically greater than 0.1 V) used for reported carbon-based sensors (Table S3 online). Therefore, the GAF has ultra-low power consumption (with the power of $\sim 4.7 \mu\text{W}$) due to its high electrical conductivity.

GAF sensors not only have the sensing performance of strain and pressure, and low power consumption, but also the potential applications in speech recognition. As is shown in Fig. 4a, the GAF sensor (110 μm thickness) can be attached on the larynx of a user with scotch tape. When the user spoke distinct words, such as “Hi”, “Good” and “Okay”, the obtained curves were distinctive

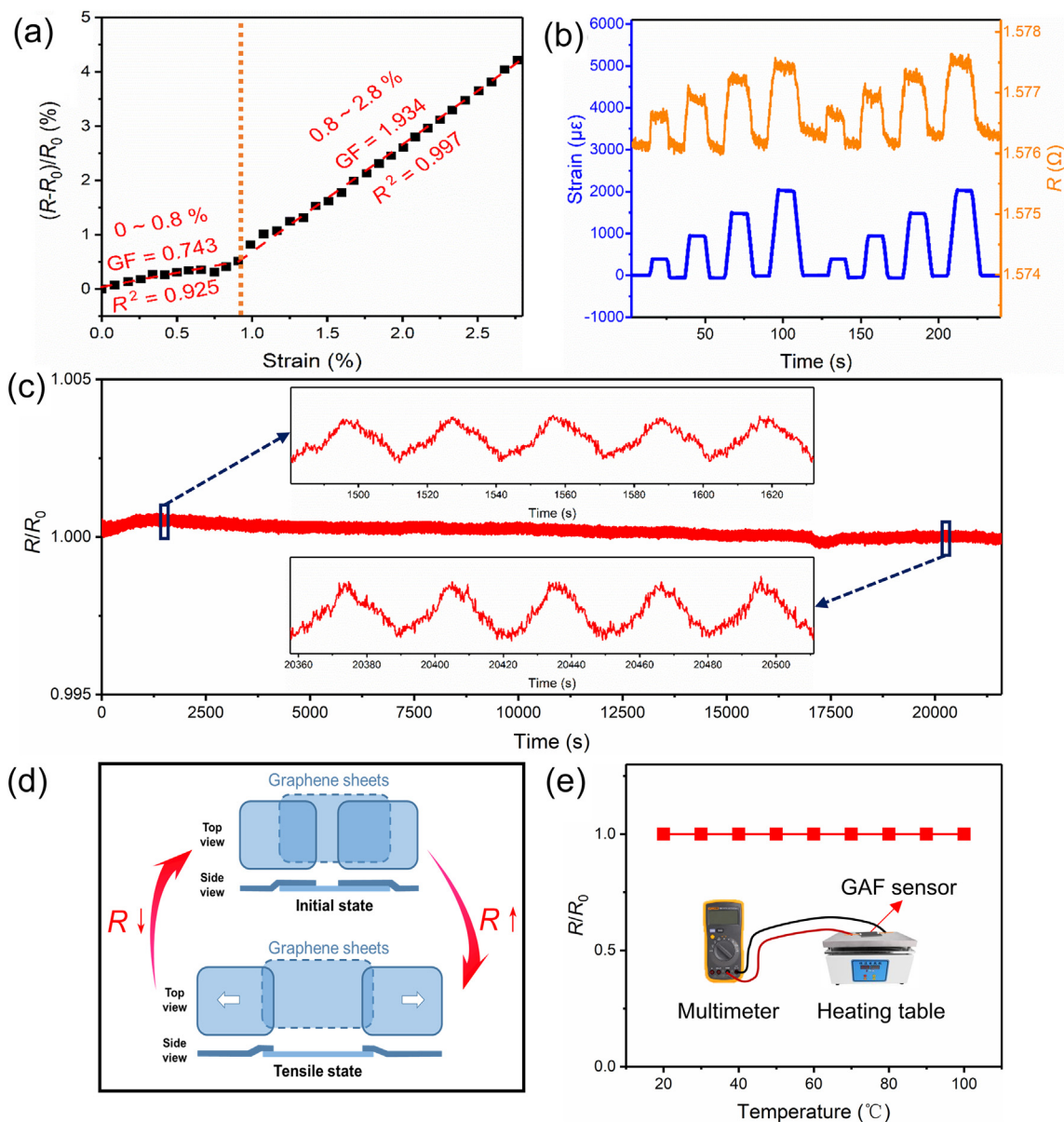


Fig. 3. (Color online) Performance, tensile cycle stability and thermal stability of the GAF strain sensor. (a) The GF and linear behavior of the GAF based strain sensor. (b) Repeated measurements of the corresponding resistance variation of the sensor with different strains. (c) Resistance variation of the GAF based strain sensor during tensile strain stretching-releasing cycles for 720 cycles under tensile strain of 0 ~ 670 μe . The insets are magnified views of resistance variations during 1480.4–1632.1 s and 20,357.6–20,511.1 s, respectively. (d) Schematic diagram of the resistance change mechanism of the GAF strain sensor during the tensile-recovery cycle testing. (e) The resistance of the GAF sensor when the temperature of the heating table was heated from 20 to 100 $^{\circ}\text{C}$.

and reproducible (Fig. 4b–d). Specifically, during the speaker's pronunciation, muscles movement and significant skin deformation around the larynx generate the interfacial shear stress between the sensor and the skin. The interfacial shear stress leads to tensile deformation and resistance increase of the GAF sensor. This property manifests the great potential of GAF sensor to apply in the fields of human–computer interaction and speech rehabilitation training. In addition, the power consumed by the GAF stress sensor at this time is only ~0.08 mW, showing ultra-low power. Interestingly, the GAF sensor (110 μm thickness) can also be applied to detect the flow of air. As shown in Fig. 4e, f, S8 (online) and Movie S2 (online), when a user blows air towards the sensor, a signal of resistance change could be observed. This is because when air was blown toward the GAF, the GAF was bent due to the fixed ends of the GAF. In this case, both sides of the GAF were subjected to tensile and compressive strains, respectively. The distribution of

strain was not uniform. Moreover, the local strain would vary along the thickness and contribute to conductivity as shown in Fig. S7g (online). The measured resistance is a combination of all these factors.

4. Conclusion

In summary, we have developed a high conductive, flexible and freestanding GAF, which is assembled by micron-sized pores and micro-fold graphene laminates during high-temperature heat treatment. This high-temperature treatment endows GAF with good thermal stability, making its resistance unchanged with increasing temperature. The prepared GAF sensors with high conductivity ($(2.32 \pm 0.08) \times 10^5 \text{ S m}^{-1}$) possess ultra-low operating voltage (0.01 V), which is much lower than the reported

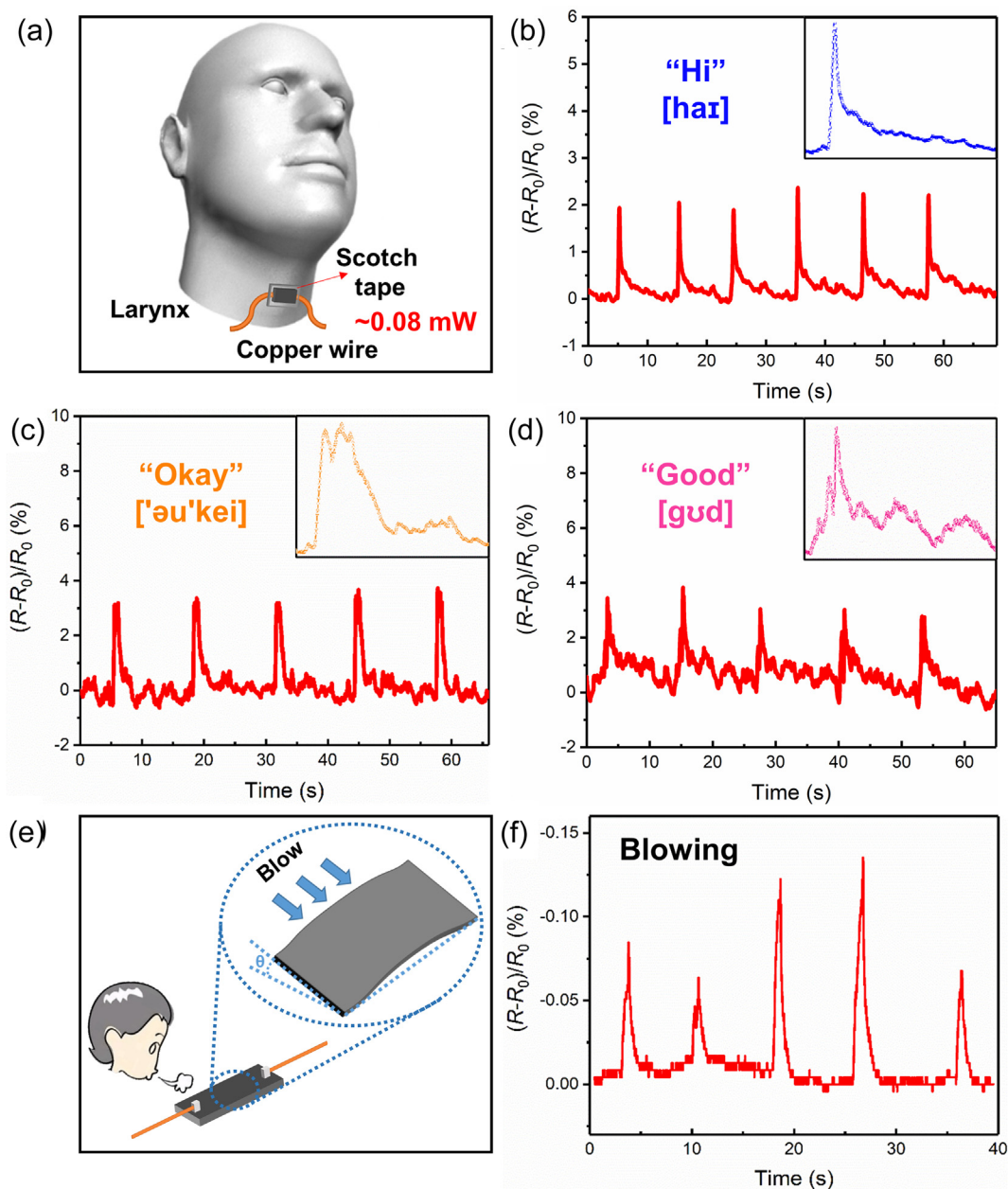


Fig. 4. (Color online) Speech recognition, air flow detecting of the GAF sensor with ultra-low power consumption. (a) The GAF sensor ($110 \mu\text{m}$ thickness) attached on the larynx of the user with scotch tape. (b–d) The corresponding obtained curves of resistance change of the GAF sensor when the user spoke words of “Hi”, “Okay” and “Good”, respectively. (e) Schematic diagram of air blowing and (f) the corresponding signal of resistance change of the GAF sensor ($110 \mu\text{m}$ thickness).

carbon-based sensors (0.1–5 V), thus achieving ultra-low power consumption ($\sim 4.7 \mu\text{W}$). Moreover, the manufacturing process of GAF sensor without any flexible substrate is simpler, more efficient and lower cost. Our work provides a new approach in the preparation of the sensitive material for freestanding sensors, and even energy-efficient flexible electronic devices.

Conflict of interest

The authors declare that they have no conflict of interest.

Acknowledgments

This work was supported by the National Natural Science Foundation of China (51701146, 51672204), the Fundamental Research

Funds for the Central Universities (WUT:2017B015), and Foundation of National Key Laboratory on Electromagnetic Environment Effects (614220504030617). The authors also acknowledge the Center for Materials Research and Analysis at the Wuhan University of Technology for TEM and image suggestions from Dr. Zhao Deng.

Author contributions

The manuscript was written through the contributions of all authors. Zhe Wang and Daping He had consideration for the idea and designed the experiments. Qianlong Wang, Shilin Yan, Lin Ren, Shichun Mu and Daping He oversaw the project progress. Zhe Wang and Peng Li performed the main experiments and analyzed the data. Rongguo Song, Wei Qian and Xianci Zeng

participated in sample fabrication. Huang Zhou and Yong Wang performed electron microscopic characterization. Zhe Wang, Huang Zhou, Peng Li, Lin Ren and Daping He wrote the manuscript.

Appendix A. Supplementary materials

Supplementary materials to this article can be found online at <https://doi.org/10.1016/j.scib.2020.05.002>.

References

- [1] Wang C, Xia K, Wang H, et al. Advanced carbon for flexible and wearable electronics. *Adv Mater* 2019;31:1801072.
- [2] Tang D, Wang Q, Wang Z, et al. Highly sensitive wearable sensor based on a flexible multi-layer graphene film antenna. *Sci Bull* 2018;63:574–9.
- [3] Yang T, Jiang X, Zhong Y, et al. A Wearable and highly sensitive graphene strain sensor for precise home-based pulse wave monitoring. *ACS Sensors* 2017;2:967–74.
- [4] Ma T, Gao H, Cong H, et al. A bioinspired interface design for improving the strength and electrical conductivity of graphene-based fibers. *Adv Mater* 2018;30:1706435.
- [5] Wang Y, Wang Y, Yang Y. Graphene-polymer nanocomposite-based redox-induced electricity for flexible self-powered strain sensors. *Adv Energy Mater* 2018;8:1800961.
- [6] Li F, Bao Y, Wang D, et al. Smartphones for sensing. *Sci Bull* 2016;61:190–201.
- [7] Roh E, Hwang B-U, Kim D, et al. Stretchable, transparent, ultrasensitive, and patchable strain sensor for human-machine interfaces comprising a nanohybrid of carbon nanotubes and conductive elastomers. *ACS Nano* 2015;9:6252–61.
- [8] Tao L, Zhang K, Tian H, et al. Graphene-paper pressure sensor for detecting human motions. *ACS Nano* 2017;11:8790–5.
- [9] Yamada T, Hayamizu Y, Yamamoto Y, et al. A stretchable carbon nanotube strain sensor for human-motion detection. *Nat Nanotechnol* 2011;6:296–301.
- [10] Lim S, Son D, Kim J, et al. Transparent and stretchable interactive human machine interface based on patterned graphene heterostructures. *Adv Funct Mater* 2015;25:375–83.
- [11] Wang Q, Jian M, Wang C, et al. Carbonized silk nanofiber membrane for transparent and sensitive electronic skin. *Adv Funct Mater* 2017;27:1605657.
- [12] Guo F, Jiang Y, Xu Z, et al. Highly stretchable carbon aerogels. *Nat Commun* 2018;9:881.
- [13] Cheng Y, Wang R, Sun J, et al. A Stretchable and highly sensitive graphene-based fiber for sensing tensile strain, bending, and torsion. *Adv Mater* 2015;27:7365–71.
- [14] Zhang Y-Z, Lee KH, Anjum DH, et al. MXenes stretch hydrogel sensor performance to new limits. *Sci Adv* 2018;4:eaat0098.
- [15] Yang Z, Pang Y, Han X, et al. Graphene textile strain sensor with negative resistance variation for human motion detection. *ACS Nano* 2018;12:9134–41.
- [16] Wang X, Liu Z, Zhang T. Flexible sensing electronics for wearable/attachable health monitoring. *Small* 2017;13:1602790.
- [17] Peng L, Xu Z, Liu Z, et al. Ultrahigh thermal conductive yet superflexible graphene films. *Adv Mater* 2017;29:1700589.
- [18] Song R, Wang Q, Mao B, et al. Flexible graphite films with high conductivity for radio-frequency antennas. *Carbon* 2018;130:164–9.
- [19] Hu X, Dou Y, Li J, et al. Buckled structures: fabrication and applications in wearable electronics. *Small* 2019;15:1804805.
- [20] Li W, Xu X, Liu C, et al. Ultralight and binder-free all-solid-state flexible supercapacitors for powering wearable strain sensors. *Adv Funct Mater* 2017;27:1702738.
- [21] Zhang M, Huang L, Chen J, et al. Ultratough, ultrastrong, and highly conductive graphene films with arbitrary sizes. *Adv Mater* 2014;26:7588–92.
- [22] Wang Z, Mao B, Wang Q, et al. Ultrahigh conductive copper/large flake size graphene heterostructure thin-film with remarkable electromagnetic interference shielding effectiveness. *Small* 2018;14:1704332.
- [23] Liu X, Tang C, Du X, et al. A highly sensitive graphene woven fabric strain sensor for wearable wireless musical instruments. *Mater Horiz* 2017;4:477–86.
- [24] Pan F, Chen S-M, Li Y, et al. 3D graphene films enable simultaneously high sensitivity and large stretchability for strain sensors. *Adv Funct Mater* 2018;28:1803221.
- [25] Liu Q, Chen J, Li Y, et al. High-performance strain sensors with fish-scale-like graphene-sensing layers for full-range detection of human motions. *ACS Nano* 2016;10:7901–6.
- [26] Luo Y, Wu D, Zhao Y, et al. Direct write of a flexible high-sensitivity pressure sensor with fast response for electronic skins. *Org Electron* 2019;67:10–8.
- [27] Wang X, Gu Y, Xiong Z, et al. Silk-molded flexible, ultrasensitive, and highly stable electronic skin for monitoring human physiological signals. *Adv Mater* 2014;26:1336–42.
- [28] Cai L, Li J, Luan P, et al. Highly transparent and conductive stretchable conductors based on hierarchical reticulate single-walled carbon nanotube architecture. *Adv Funct Mater* 2012;22:5238–44.
- [29] Jeong YR, Park H, Jin SW, et al. Highly stretchable and sensitive strain sensors using fragmented graphene foam. *Adv Funct Mater* 2015;25:4228–36.
- [30] Zhang R, Hu R, Li X, et al. A bubble-derived strategy to prepare multiple graphene-based porous materials. *Adv Funct Mater* 2018;28:1705879.
- [31] Karim N, Afroj S, Tan S, et al. Scalable production of graphene-based wearable E-textiles. *ACS Nano* 2017;11:12266–75.
- [32] He Z, Chen W, Liang B, et al. Capacitive pressure sensor with high sensitivity and fast response to dynamic interaction based on graphene and porous nylon networks. *ACS Appl Mater Interfaces* 2018;10:12816–23.
- [33] Boland CS, Khan U, Backes C, et al. Sensitive, high-strain, high-rate bodily motion sensors based on graphene-rubber composites. *ACS Nano* 2014;8:8819–30.
- [34] Kang D, Pikhitsa PV, Choi YW, et al. Ultrasensitive mechanical crack-based sensor inspired by the spider sensory system. *Nature* 2014;516:222–6.
- [35] Li L, Xiang H, Xiong Y, et al. Ultrastretchable fiber sensor with high sensitivity in whole workable range for wearable electronics and implantable medicine. *Adv Sci* 2018;5:1800558.
- [36] Li X, Yang T, Yang Y, et al. Large-area ultrathin graphene films by single-step marangoni self-assembly for highly sensitive strain sensing application. *Adv Funct Mater* 2016;26:1322–9.
- [37] Sheng L, Liang Y, Jiang L, et al. Bubble-decorated honeycomb-like graphene film as ultrahigh sensitivity pressure sensors. *Adv Funct Mater* 2015;25:6545–51.
- [38] Lv L, Zhang P, Xu T, et al. Ultrasensitive pressure sensor based on an ultralight sparkling graphene block. *ACS Appl Mater Interfaces* 2017;9:22885–92.
- [39] Li J, Zhao S, Zeng X, et al. Highly stretchable and sensitive strain sensor based on facilely prepared three-dimensional graphene foam composite. *ACS Appl Mater Interfaces* 2016;8:18954–61.
- [40] Kim T, Park J, Sohn J, et al. Bioinspired, highly stretchable, and conductive dry adhesives based on 1D–2D hybrid carbon nanocomposites for all-in-one ECG electrodes. *ACS Nano* 2016;10:4770–8.
- [41] Lee SM, Byeon HJ, Lee JH, et al. Self-adhesive epidermal carbon nanotube electronics for tether-free long-term continuous recording of biosignals. *Sci Rep* 2015;4:6074.
- [42] Liang H-W, Guan Q-F, Zhu Z, et al. Highly conductive and stretchable conductors fabricated from bacterial cellulose. *NPG Asia Mater* 2012;4:e19.
- [43] Kim KH, Vural M, Islam MF. Single-walled carbon nanotube aerogel-based elastic conductors. *Adv Mater* 2011;23:2865–9.
- [44] Yapici MK, Alkhidir T, Samad YA, et al. Graphene-clad textile electrodes for electrocardiogram monitoring. *Sensors Actuators B Chem* 2015;221:1469–74.
- [45] Chen Z, Ren W, Gao L, et al. Three-dimensional flexible and conductive interconnected graphene networks grown by chemical vapour deposition. *Nat Mater* 2011;10:424–8.
- [46] Sekitani T, Nakajima H, Maeda H, et al. Stretchable active-matrix organic light-emitting diode display using printable elastic conductors. *Nat Mater* 2009;8:494–9.
- [47] Lipomi DJ, Vosgueritchian M, Tee BC-K, et al. Skin-like pressure and strain sensors based on transparent elastic films of carbon nanotubes. *Nat Nanotechnol* 2011;6:788–92.
- [48] Park H, Kim JW, Hong SY, et al. Microporous polypyrrole-coated graphene foam for high-performance multifunctional sensors and flexible supercapacitors. *Adv Funct Mater* 2018;28:1707013.



Zhe Wang is a Ph.D. candidate at School of Science, Wuhan University of Technology (WUT). He received his B.S. and M.S. degrees at School of Chemical and Biological Engineering in Changsha University of Science & Technology (2015) and State Key Laboratory of Advanced Technology for Materials Synthesis and Processing in WUT (2018), respectively. His research is mainly focused on graphene-based film materials for electromagnetic interference shielding, strain sensors and mechanics.



Peng Li is an experimentalist at WUT. He received his M.S. degree in Radio Physics, and Ph.D. degree in Engineering Mechanics in WUT. His research interests are structural health monitoring, sensor technology and experimental mechanics.



Lin Ren is an associate professor at WUT. She obtained her Ph.D. degree in Material Processing Engineering from WUT in 2015. Her research interests include the preparation and application of nano-materials and ceramic matrix composites.



Daping He is a full professor at WUT. He obtained his Ph.D. degree in Materials Processing Engineering from WUT in 2013. He was a postdoctoral fellow in the University of Science and Technology of China. Then he joined University of Bath as a Newton International Fellow and University of Cambridge as a postdoctoral fellow. His research interest is preparation and application of nano-composite materials into new energy devices, sensors and RF microwaves field.